Trends in Computational and Applied Mathematics, **24**, N. 2 (2023), 265-274
Sociedade Brasileira de Matemática Aplicada e Computacional
Online version ISSN 2676-0029
www.scielo.br/tcam
doi: 10.5540/tcam.2023.024.02.00265

Stagnation Points Beneath Rotational Solitary Waves in Gravity-Capillary Flows

M. V. FLAMARION

Received on April, 10 2022 / Accepted on September 19, 2022

ABSTRACT. Stagnation points beneath solitary gravity-capillary waves in the weakly nonlinear weakly dispersive regime in a sheared channel with finite depth and constant vorticity are investigated. A Korteweg-de Vries equation that incorporates the surface tension and the vorticity effects is obtained asymptotically from the full Euler equations. The velocity field in the bulk fluid is approximated which allow us to compute stagnation points in the solitary wave moving frame. We show that stagnation points bellow the crest of elevation solitary waves exist for large values of the vorticity and Bond numbers less than a critical value that depends on the vorticity. Remarkably, the positions of these stagnation points do not depend on the surface tension. Besides, we show that when there are two stagnation points located at the bottom of the channel, they are pulled towards the horizontal coordinate of the solitary wave crest as the Bond number increases until its critical value.

Keywords: gravity-capillary waves, Euler equations, KdV equation, stagnation points.

1 INTRODUCTION

Particle trajectories beneath gravity water waves have been studied ever since Stokes [17] (1847). Our understanding of this problem has developed quite a bit since then. There have been many numerical and theoretical works on particle trajectories using different frameworks and therefore it is hard to give a comprehensive overview of contributions. For the interested reader, we summarize here some works in which this problem has been studied.

Stokes [17] showed that for periodic surface waves in the shallow water and deep water regime, the particle trajectories follow loops with a mean Stokes' drift (small horizontal displacement) in the wave propagation direction. Consequently, he concluded that in the presence of a counter-current closed orbits always exist. However, the successive approximation method used in his work lacked of mathematical rigour. A rigorous proof of the Stokes' drift existence in the shallow water and deep water regime was given by Ursell [19]. Only recently, Constantin and Villari [4]

UFRPE/Rural Federal University of Pernambuco, UACSA/Unidade Acadêmica do Cabo de Santo Agostinho, BR 101 Sul, 5225, 54503-900, Ponte dos Carvalhos, Cabo de Santo Agostinho, Pernambuco, Brazil – E-mail: marcelo.flamarion@ufrpe.br https://orcid.org/0000-0001-5637-7454

proved the nonexistence of closed orbits for the linear problem and Constantin and Strauss [5] proved that it is always possible to find closed orbits in the presence of a uniform counter-current. Notwithstanding, the position of the particles that describe closed orbits were not determined. These orbits were later computed numerically by Nachbin and Ribeiro-Jr [14] using a boundary integral method for the full Euler equations. Particle trajectories have also been computed numerically using asymptotic models such as the Korteweg-de Vries equation (KdV) [1, 2, 8, 9], Serre equations [12] and Schrödinger equation [3, 6].

In the presence of a linear sheared current and in the moving frame of the water surface the dynamical system of particle trajectories becomes autonomous and the flow structure can be seen through the streamlines. In this case, an interesting flow structure so-called Kelvin cat-eyes arises. This structure is featured by the existence of stagnation points (critical points of the autonomous dynamical system) and closed streamlines. Using the full Euler equations, Teles Da Silva and Peregrine [18] used a boundary integral formulation to capture closed streamlines. Related results and anomalies in the pressure in the bulk fluid were later reported by Ribeiro-Jr et al. [15] using the conformal mapping method and a time-dependent Kelvin cat-eye structure over a variable topography was captured by Flamarion et al. [7] for the linear problem. Similar results with respect to solitary waves for the KdV equation was also obtained by Johnson [11] using an asymptotic method. More recently, Guan [9] used the Korteweg-de Vries equation to compute closed streamlines beneath solitary waves. He showed that the KdV predictions agree well with the full Euler equations for solitary waves with small amplitudes.

When surface tension is included to the full Euler equations, Martin [13] proved the existence of steady periodic equatorial geophysical water waves with capillary effects and stagnation points. He also showed that if the vorticity is large enough these flows possess stagnation points. Hur and Wheeler [10] found Kelvin cat-eye streamline patterns beneath Crapper's capillary waves in a rotational flow with constant vorticity. Stagnation points for periodic pure capillary waves and gravity-capillary waves were also found in the recent work of Shoji and Okamoto [16]. To the best of our knowledge there are no articles studying the submarine Kelvin cat-eye structure and stagnation points beneath solitary waves for KdV equation in the presence of surface tension.

In this work, our goal is to investigate the role of the surface tension on particle trajectories beneath gravity-capillary solitary waves in the presence of a vertically sheared current with constant vorticity. More precisely, we are interested in studying the effects of the surface tension on stagnation points. We focus on gravity-capillary waves in the weakly nonlinear, weakly dispersive regime. Under these assumptions, we derive a Korteweg-de Vries equation that incorporates the surface tension and the vorticity effects asymptotically from the full Euler equations. This allow us to approximate the velocity field in the bulk fluid and consequently compute particle trajectories. The problem is reformulated in the moving frame of elevation solitary waves and stagnation points are found bellow their crests for large values of the vorticity and for Bond numbers less than a critical value that depends on the vorticity. Furthermore, we show that the position of these stagnation points do not depend on the surface tension. In addition, we show that when there are two stagnation points at the bottom of the channel, they are pulled towards

the horizontal coordinate of the solitary wave crest as the Bond number increases until its critical value.

2 MATHEMATICAL FORMULATION

In this section, we present the mathematical formulation of the problem and derive asymptotically a KdV equation for rotational gravity-capillary solitary waves.

We consider a two-dimensional incompressible flow of an inviscid fluid with constant density (ρ) in a finite depth channel (h) with constant vorticity ($-\omega$) under the gravity force (g) and surface tension (σ). Under these assumptions the velocity field in the bulk fluid can be written as

$$\nabla\tilde{\phi}(x,y,t)+(\omega y,0), \tag{2.1}$$

where $\tilde{\phi}(x,y,t)$ is the harmonic component of the velocity field. The governing equations that model the problem are the full Euler equations

$$\tilde{\phi}_{xx}+\tilde{\phi}_{yy}=0 \text{ for } -h<y<\tilde{\eta}(x,t), \tag{2.2}$$

$$\tilde{\phi}_{y}=0 \text{ at } y=-h, \tag{2.3}$$

$$\tilde{\eta}_{t}+\eta_{x}\Big(\omega\tilde{\eta}+\tilde{\phi}_{x}\Big)-\tilde{\phi}_{y}=0 \text{ at } y=\tilde{\eta}(x,t), \tag{2.4}$$

$$\tilde{\phi}_{t}+\frac{1}{2}\Big(\tilde{\phi}_{x}^{2}+2\omega\tilde{\eta}\tilde{\phi}_{x}+\tilde{\phi}_{y}^{2}\Big)+g\tilde{\eta}-\omega\tilde{\psi}-\frac{\sigma}{\rho}\frac{\tilde{\eta}_{xx}}{(1+\tilde{\eta}_{x}^{2})^{3/2}}=0 \text{ at } y=\tilde{\eta}(x,t), \tag{2.5}$$

where $\tilde{\psi}$ is the harmonic conjugate of $\tilde{\phi}$ and $\tilde{\eta}$ is the free surface. It is convenient to rewrite the system (2.2)-(2.5) using dimensionless variables. To this end, we consider λ as a typical wavelength, a as a typical wave amplitude, $c_0=(gh)^{1/2}$ the linear long-wave speed and introduce the scaling

$$x\to\lambda x,\ \ y\to hy,\ \ t\to\frac{\lambda}{c_0}t,\ \ \tilde{\eta}=a\eta,\ \ \tilde{\phi}=\frac{ac_0\lambda}{h}\phi,\ \ \tilde{\psi}=ac_0\psi. \tag{2.6}$$

Sustituting (2.6) in (2.2)-(2.5) we obtain the following set of dimensionless equations

$$\mu^{2}\phi_{xx}+\phi_{yy}=0 \text{ for } -1<y<\varepsilon\eta(x,t), \tag{2.7}$$

$$\tilde{\phi}_{y}=0 \text{ at } y=-1, \tag{2.8}$$

$$\eta_{t}+\varepsilon\eta_{x}\Big(\Omega\eta+\phi_{x}\Big)-\frac{1}{\mu^{2}}\phi_{y}=0 \text{ at } y=\varepsilon\eta(x,t), \tag{2.9}$$

$$\tilde{\phi}_{t}+\frac{\varepsilon}{2}\Big(\phi_{x}^{2}+2\Omega\eta\phi_{x}+\frac{1}{\mu^{2}}\phi_{y}^{2}\Big)+\eta-\Omega\psi-\frac{\mu^{2}B\eta_{xx}}{(1+\varepsilon^{2}\mu^{2}\eta_{x}^{2})^{3/2}}=0 \text{ at } y=\varepsilon\eta(x,t), \tag{2.10}$$

where $\varepsilon=a/h$ is the nonlinearity parameter, $\mu=h/\lambda$ is the shallow water parameter, $-\Omega=-\omega h/c_0$ is the dimensionless vorticity and $B=\sigma/\rho gh^{2}$ is the Bond number. We point out that when $B\neq 0$ the dynamic of the free surface is controlled by the effects of the surface tension and by fluid inertia. On the other hand, when $B=0$, the dynamic is fully dominated by fluid inertia [20].

In order to obtain an asymptotic model from equations (2.7)-(2.10), the weakly nonlinear ($\varepsilon \approx 0$) weakly dispersive ($\mu^2 \approx 0$) regime is considered. Moreover, we assume that nonlinearity and dispersion are balanced as $\varepsilon = \mu^2$ and that the potential velocity is given by the power series expansion [20]

$$\phi(x,y,t) = \sum_{n=0}^{\infty} f_n(x,t)(y+1)^n. \tag{2.11}$$

Substituting equation (2.11) in condition (2.7), we formally obtain

$$\begin{aligned} 0 = \varepsilon\phi_{xx} + \phi_{yy} &= \sum_{n=0}^{\infty} \varepsilon\partial_x^2 f_n(x,t)(y+1)^n + \sum_{n=2}^{\infty} n(n-1) f_n(x,t)(y+1)^n \\ &= \sum_{n=0}^{\infty} \Big(\varepsilon\partial_x^2 f_n(x,t) + (n+2)(n+1) f_{n+2}(x,t)\Big)(y+1)^n. \end{aligned} \tag{2.12}$$

Thus, after some algebra we have the following expression for the potential velocity

$$\phi(x,y,t) = \sum_{n=0}^{\infty} (-1)^n \frac{\varepsilon^n}{(2n)!} \frac{\partial^{2n} f_0}{\partial x^{2n}} (y+1)^{2n} + \sum_{n=0}^{\infty} (-1)^n \frac{\varepsilon^n}{(2n+1)!} \frac{\partial^{2n+1} f_1}{\partial x^{2n+1}} (y+1)^{2n+1}. \tag{2.13}$$

From the Neumann condition (2.8) we conclude that $f_1(x,t) \equiv 0$. Consequently, the potential velocity and its harmonic conjugate can be written as

$$\phi(x,y,t) = \sum_{n=0}^{\infty} (-1)^n \frac{\varepsilon^n}{(2n)!} \frac{\partial^{2n} \mathbf{\Phi}}{\partial x^{2n}} (y+1)^{2n}, \tag{2.14}$$

$$\psi(x,y,t) = \sum_{n=0}^{\infty} (-1)^n \frac{\varepsilon^n}{(2n+1)!} \frac{\partial^{2n+1} \mathbf{\Phi}}{\partial x^{2n+1}} (y+1)^{2n+1}, \tag{2.15}$$

where $\mathbf{\Phi}(x,t) = \phi(x,-1,t)$ is the potential velocity evaluated at the bottom of the channel. Substituting equations (2.14)-(2.15) into Kinematic and Bernoulli conditions (2.8)-(2.9) and neglecting the second order terms as done by Guan [9] we obtain

$$\begin{aligned} &\mathbf{\Phi}_{tt} - \mathbf{\Phi}_{xx} - \Omega\mathbf{\Phi}_{tx} - \varepsilon\Big[\eta_x\mathbf{\Phi}_x + \Omega\eta\eta_x + \eta\mathbf{\Phi}_{xx}\Big] \\ &- \varepsilon\Big[\frac{1}{2}\mathbf{\Phi}_{ttxx} - \frac{1}{2}\big(\mathbf{\Phi}_x^2\big)_t - \frac{\Omega}{6}\mathbf{\Phi}_{txxx} - \frac{1}{6}\mathbf{\Phi}_{xxxx}\Big] - \varepsilon B\eta_{xxt} = 0. \end{aligned} \tag{2.16}$$

Notice that substituting equation (2.13) into (2.10) we obtain

$$\eta = -\mathbf{\Phi}_t + \Omega\mathbf{\Phi}_x + \mathscr{O}(\varepsilon), \tag{2.17}$$

then using this fact in equation (2.16) yields

$$\begin{aligned} &\mathbf{\Phi}_{tt} - \mathbf{\Phi}_{xx} - \Omega\mathbf{\Phi}_{tx} - \varepsilon\Big[\eta_x\mathbf{\Phi}_x + \Omega\eta\eta_x + \eta\mathbf{\Phi}_{xx}\Big] \\ &- \varepsilon\Big[\Big(\frac{1}{2} - B\Big)\mathbf{\Phi}_{ttxx} - \frac{1}{2}\big(\mathbf{\Phi}_x^2\big)_t - \Big(\frac{\Omega}{6} - \Omega B\Big)\mathbf{\Phi}_{txxx} - \frac{1}{6}\mathbf{\Phi}_{xxxx}\Big] = 0. \end{aligned} \tag{2.18}$$

In an effort to obtain an asymptotic model for right-going traveling waves, we introduce the new variables $\xi = x - ct$ and $\tau = \varepsilon t$, where c is the solution of $c^2 + \Omega c = 1$ on the positive branch, i.e.,

$$c = -\frac{\Omega}{2} + \frac{\sqrt{\Omega^2+4}}{2}. \tag{2.19}$$

Denote by $\mathbf{\Phi}(\xi,\tau)$ and $\eta(\xi,\tau)$ the potential velocity evaluated at the bottom of the channel and the free surface in the new coordinate system respectively. Thus,

$$\mathbf{\Phi}_x = \mathbf{\Phi}_\xi, \tag{2.20}$$

$$\mathbf{\Phi}_t = -c\mathbf{\Phi}_\xi + \varepsilon\mathbf{\Phi}_\tau, \tag{2.21}$$

$$\mathbf{\Phi}_{tt} = c^2\mathbf{\Phi}_{\xi\xi} - 2c\varepsilon\mathbf{\Phi}_{\xi\tau} + \mathscr{O}(\varepsilon^2), \tag{2.22}$$

$$\mathbf{\Phi}_{xt} = -c\mathbf{\Phi}_{\xi\xi} + \varepsilon\mathbf{\Phi}_{\xi\tau}. \tag{2.23}$$

In particular, from equation (2.17) we have

$$\eta = (c+\Omega)\mathbf{\Phi}_\xi + \mathscr{O}(\varepsilon). \tag{2.24}$$

Substituting the relations (2.20)-(2.23) into (2.18) after some algebra we have

$$\mathbf{\Phi}_{\xi\tau} + \frac{(\Omega^2+3)(c+\Omega)}{2c+\Omega}\mathbf{\Phi}_\xi\mathbf{\Phi}_{\xi\xi} + \Big(\frac{c^2}{3(2c+\Omega)} - \frac{B}{2c+\Omega}\Big)\mathbf{\Phi}_{\xi\xi\xi\xi} = 0. \tag{2.25}$$

Using equation (2.24) in equation (2.25) yields the Korteweg-de Vries equation that incorporates both, the surface tension and vorticity effects

$$\eta_\tau + \alpha\eta\boldsymbol{\eta}_\xi + \beta\eta_{\xi\xi\xi} = 0, \text{ where } \alpha = \frac{\Omega^2+3}{2c+\Omega} \text{ and } \beta = \Big(\frac{c^2}{3(2c+\Omega)} - \frac{B}{2c+\Omega}\Big). \tag{2.26}$$

It is worth to mention that the dispersive term of this KdV equation vanishes when $B = B_c \equiv c^2/3$. This critical value as a function of the vorticity parameter is depicted in Figure 1. Traveling sech^2–like solutions for equation (2.26) only exists when $B \neq B_c$. In addition, elevation solitary wave solutions of (2.26) occur when $0 \leq B < B_c$ and depression solitary wave solutions of (2.26) occur when $B > B_c$. From this point on, we focus only on elevation solitary waves ($0 \leq B < B_c$).

Solitary wave solutions of (2.26) are described by the formula [20]

$$\eta(\xi,\tau) = A\,\text{sech}^2(k(\xi - C\tau)), \text{ where } k = \sqrt{\frac{\alpha A}{12\beta}} \text{ and } C = \frac{\alpha A}{3}. \tag{2.27}$$

Consequently, from equation (2.24) we obtain

$$\mathbf{\Phi}_\xi(\xi,\tau) = \frac{A}{c+\Omega}\,\text{sech}^2(k(\xi - C\tau)). \tag{2.28}$$

Once we are interested in investigating particle trajectories for the full model using the KdV model as an approximation, we have to express the free surface and the potential velocity using the Euler coordinates. The solitary wave solution in Euler coordinates is

$$\eta(x,t) = A\,\text{sech}^2\Big(k(x - (c+\varepsilon C)t)\Big), \text{ where } k = \sqrt{\frac{\alpha A}{12\beta}} \text{ and } C = \frac{\alpha A}{3}, \tag{2.29}$$

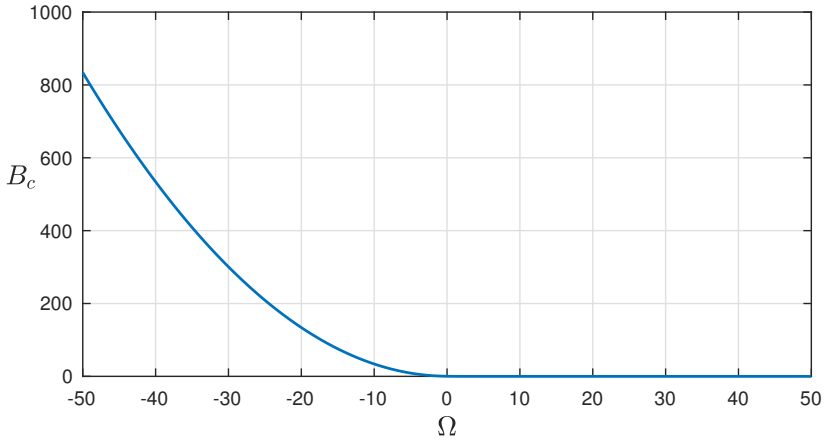

Figure 1: The critical value of the Bond number (B_c) as a function of the vorticity parameter (Ω).

and the horizontal velocity evaluated at the bottom of the channel is

$$\mathbf{\Phi}_x(x,t) = \frac{A}{c+\Omega}\,\mathrm{sech}^2\Big(k(x-(c+\varepsilon C)t)\Big). \tag{2.30}$$

3 COMPUTING PARTICLE TRAJECTORIES

In this section we formulate the dynamical system of particles in the bulk fluid and investigate the role of the surface tension on the particle trajectories.

Particle trajectories beneath the solitary wave (2.29) can be computed approximately by solving the dynamical system

$$\frac{dx}{dt} = \Omega y + \varepsilon\phi_x(x,y,t) \approx \Omega y + \varepsilon\mathbf{\Phi}_x(x,t), \tag{3.1}$$

$$\frac{dy}{dt} = \phi_y(x,y,t) \approx -\varepsilon\mathbf{\Phi}_{xx}(x,t)(y+1). \tag{3.2}$$

In order to compute stagnation points, it is convenient to solve (3.1)-(3.2) rewriting the horizontal speed at the bottom of the channel (2.30) in the wave moving frame $X = x-(c+\varepsilon C)t$ and $Y = y$. In this new framework, particle trajectories are solutions of the autonomous dynamical system

$$\frac{dX}{dt} = \Omega Y - (c+\varepsilon C) + \varepsilon\mathbf{\Phi}_X(X), \tag{3.3}$$

$$\frac{dY}{dt} = -\varepsilon\mathbf{\Phi}_{XX}(X)(Y+1), \tag{3.4}$$

which are represented by the streamlines i.e., particle trajectories are the level curves of the stream function $\mathbf{\Psi}(X,Y)$, which is given by

$$\mathbf{\Psi}(X,Y) = \varepsilon\mathbf{\Phi}_X(X)(Y+1) + \frac{\Omega}{2}Y^2 - (c+\varepsilon C)Y. \tag{3.5}$$

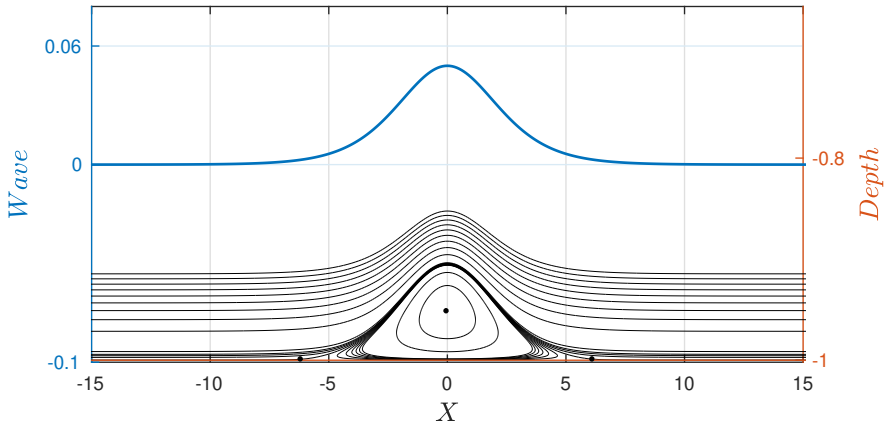

Figure 2: Typical phase portrait of (3.3)-(3.4) for a linear sheared current with $A = 0.5$, $\Omega = -20$ and $B = 0.5$. The dots represent the position of the stagnation points.

The streamlines (3.5) are computed using the function *contour* that is implemented in MATLAB.

In the absence of surface tension, Guan [9] investigated particle trajectories beneath solitary waves in the presence of a linear sheared current through the Korteweg-de Vries equation. He showed that the orbits obtained from the asymptotic approximation agree well with the ones computed through the full Euler equations when the solitary waves have small amplitudes. Based on his results, in all simulations presented in this article we fix $\varepsilon = 0.1$. A typical phase portrait of (3.3)-(3.4) is shown in Figure 2.

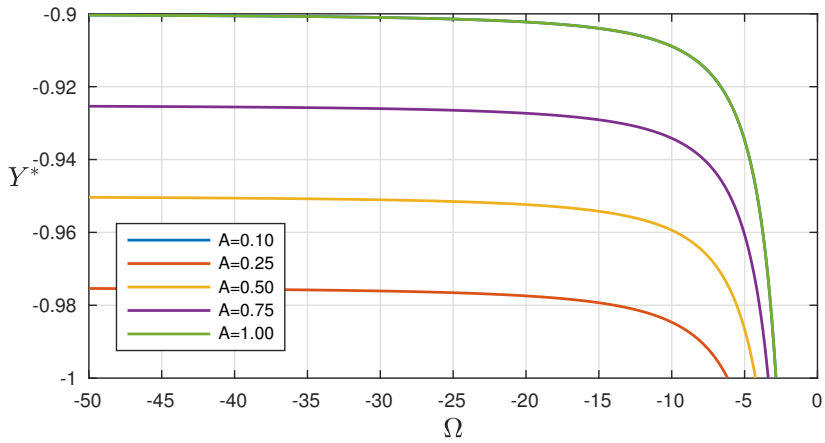

Figure 3: The vertical coordinate of the stagnation point $(0, Y^*)$ as a function of the vorticity parameter for different values of an amplitude of the solitary wave (2.29).

We find stagnation points for large values of the vorticity parameter beneath elevation solitary waves with $0 \leq B < B_c$. It is remarkable that the presence of surface tension does not change the position of the stagnation points bellow the crest of the solitary wave. Denoting by $(0, Y^*)$ the coordinates of a stagnation point bellow the crest of a solitary wave (2.29), we see that the vertical coordinate Y^* satisfies the equation

$$0 = \Omega Y^* - (c + \varepsilon C) + \varepsilon \mathbf{\Phi}_X(0) = \Omega Y^* - (c + \varepsilon C) + \frac{\varepsilon A}{c + \Omega}, \tag{3.6}$$

which only depends on the vorticity parameter and on the amplitude of the solitary wave, but not on the surface tension. Figure 3 displays the vertical coordinate of these stagnation points (Y^*) as a function of the vorticity parameter for different values of the amplitude of the solitary wave (2.29). Notice that the stagnation point appears initially at the bottom of the channel for a critical value of the vorticity and once the vorticity increases the stagnation points move upwards. Nonetheless, all stagnation points remain located close to the bottom of the channel. Besides, solitary waves of small amplitudes require stronger vorticity values so that stagnation points can arise.

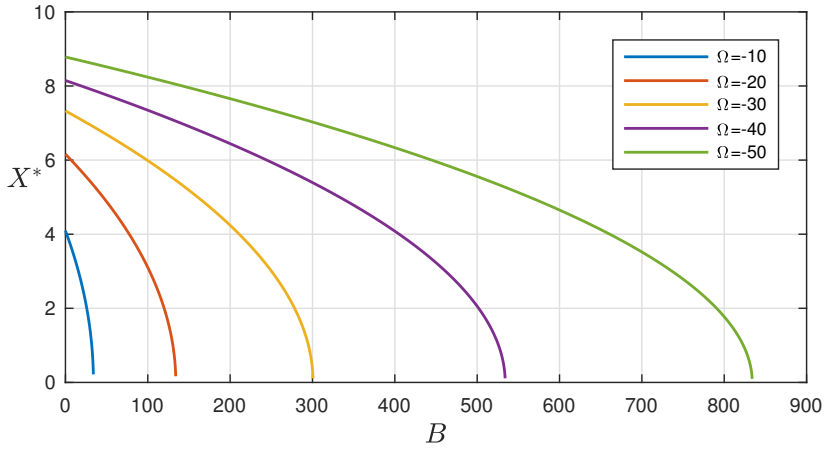

Figure 4: The horizontal coordinate of the stagnation point $(X^*, -1)$ as a function of the Bond number for different values of the vorticity parameter and amplitude $A = 0.5$.

There are also regimes in which two stagnation points symmetric with respect to the $y-$axis exist at the bottom of the channel. Denote these two stagnation points by $(\pm X^*, -1)$ with $X^* > 0$. Therefore, the horizontal coordinate X^* is obtained by solving the equation

$$0 = -\Omega - (c + \varepsilon C) + \varepsilon \mathbf{\Phi}_X(X^*) = -\Omega - (c + \varepsilon C) + \frac{\varepsilon A}{c + \Omega} \operatorname{sech}^2(kX^*) = 0. \tag{3.7}$$

Differently from the stagnation point bellow the solitary wave crest, in this case the surface tension affects its position. In fact, we notice that the point X^* approaches zero as $B \to B_c$. In addition, for a fixed value of Ω, the coordinate X^* decreases as a function of the Bond number

(B). More details of these dependences are depicted in Figure 4 for a fixed value of the solitary wave amplitude.

4 CONCLUSIONS

In this paper, we have obtained a Korteweg-de Vries equation for gravity-capillary waves in the presence of a vertically sheared current with constant vorticity using asymptotic analysis for the full Euler equations. We computed numerically stagnation points that are beneath the crest of elevation solitary waves for large values of the vorticity and Bond number in the range $0 \leq B < B_c$. In addition, we showed that the surface tension does not affect the position of these stagnation points. Besides, we showed that when there are two stagnation points located at the bottom of the channel, they are pulled towards the horizontal coordinate of the solitary wave crest as the Bond number increases until its critical value. It would be interesting to investigate the existence of stagnation points when the Bond number is critical. However, the asymptotic model deduced in this article is not appropriate for this study. An attempt to obtain a higher-order KdV model that incorporates the surface tension and vorticity effects seems a natural path to be pursued in future.

Acknowledgments

The author is grateful to the unknown referees for their constructive comments and suggestions which improved the manuscript.

REFERENCES

[1] A. Alfatih & H. Kalisch. Reconstruction of the pressure in long-wave models with constant vorticity. *Eur J Mech B-Fluid*, **37** (2013), 187–194.

[2] H. Borluk & H. Kalisch. Particle dynamics in the kdv approximation. *Wave Motion*, **49** (2012), 691–70.

[3] J. Carter, C. Curtis & H. Kalisch. Particle trajectories in nonlinear Schrödinger models. *Water Waves*, **2** (2020), 31–57.

[4] A. Constantin & G. Villari. Particle trajectories in linear water waves. *J Math Fluid Mech*, **10** (2008), 1336–1344.

[5] A. Constantin & S. W. Pressure beneath a Stokes wave. *Comm Pure Appl Math*, **63** (2010), 533–557.

[6] C. Curtis, J. Carter & H. Kalisch. Particle paths in nonlinear schrödinger models in the presence of linear shear currents. *J Fluid Mech*, **885** (2018), 322–350.

[7] M.V. Flamarion, A. Nachbin & R. Ribeiro-Jr. Time-dependent Kelvin cat-eye structure due to current-topography interaction. *J Fluid Mech*, **889**(A11) (2020).

[8] L. Gagnon. Qualitative description of the particle trajectories for n-solitons solution of the korteweg-de vries equation. *Discrete Contin Dyn Syst*, **37** (2017), 1489–1507.

[9] X. Guan. Particle trajectories under interactions between solitary waves and a linear shear current. *Theor App Mech Lett*, **10** (2020), 125–1131.

[10] V. Hur & M. Wheeler. Exact free surfaces in constant vorticity flows. *J Fluid Mech*, **896**(R1) (2020).

[11] R.S. Johnson. On the nonlinear critical layer below a nonlinear unsteady surface wave. *J Fluid Mech*, **167** (1986), 327–351.

[12] Z. Khorsand. Particle trajectories in the Serre equations. *Appl Math Comput*, **230** (2014), 35–42.

[13] C.I. Martin. Equatorial wind waves with capillary effects and stagnation points. *Nonlinear Anal-Theor*, **96** (2014), 1–8.

[14] A. Nachbin & R. Ribeiro-Jr. A boundary integral method formulation for particle trajectories in Stokes Waves. *DCDS-A*, **34**(8) (2014), 3135–3153.

[15] R. Ribeiro-Jr, A. Milewski P & A. Nachbin. Flow structure beneath rotational water waves with stagnation points. *J Fluid Mech*, **812** (2017), 792–814.

[16] M. Shoji & H. Okamoto. Stationary water waves on rotational flows of two vortical layers. *Jpn J Ind Appl Math*, **38** (2021), 79–103.

[17] G.G. Stokes. On the theory of oscillatory waves. *Trans Cambridge Phil Soc*, **41**(8) (1847), 441–455.

[18] F. Teles Da Silva, A & H. Peregrine, D. Steep, steady surface waves on water of finite depth with constant vorticity. *J Fluid Mech*, **195** (1988), 281–302.

[19] F. Ursell. Mass transport in gravity waves. *Proc Cambridge Phil Soc*, **40** (1953), 145–150.

[20] G.B. Whitham. “Linear and Nonlinear Waves”. Wiley (1974).